Formation of a mesh-like electrodeposit induced by electroconvection

Mu Wang*†, Willem J. P. van Enckevort*, Nai-ben Ming† & Piet Bennema*

* RIM, Laboratory of Solid State Chemistry, Faculty of Science, University of Nijmegen, 6525 ED Nijmegen, The Netherlands
† National Laboratory of Solid State Microstructures, Nanjing University, Nanjing 210008, China

ELECTRODEPOSITION of metals such as copper and zinc from solutions of their salts may give rise to ramified metal deposits which show a range of growth morphologies[1–9]. Our understanding of the factors that determine growth morphology is still very limited, in part because different morphologies may be observed even under similar growth conditions[4,5]. It is thought[9] that uncontrolled convective processes at the tips of the deposit branches may play a role in these discrepancies. Here we show that convective effects, which we can visualize directly, in the electrodeposition of iron from $FeSO_4$ solution, can generate a mesh-like pattern, a morphology that has not been reported previously. Convection can be diminished by altering the pH, whereupon we see a transition to a dense branching morphology. Our results show that convective effects do indeed play an important part in determining pattern selection during electrodeposition.

The metal deposit formed in electrodeposition from acidified $FeSO_4$ aqueous solution film (Fig. 1) and its evolution process (Fig. 2) are studied using an *in situ* observation method. Unlike the fractal-like or dendritic patterns observed previously[1–6,10], in our experiment the neighbouring tips of the deposit branches approach each other and form a mesh-like pattern. In order to find out the possible mechanism behind this phenomenon, interference contrast microscopy, a method capable of mapping gradients in concentration, is employed to investigate the concentration profile near the growing interface (Fig. 3). Bright arches, which signify local concentration gradients, are found connecting the neighbouring branches. Moreover, the tips of the deposit branches approach each other along the arch. The curvature and the contrast of the arch decrease during this process (Fig. 3*a–d*). We have found that observation of this phenomenon requires sufficient H_3O^+ concentration in the electrolyte solution: if no sulphuric acid is added to the $FeSO_4$ solution initially, the mesh-like pattern is not observed, the morphology instead being densely branched.[11] Additionally, in electrodeposition of acidified $FeSO_4$ solution, when the mesh-like pattern grows for some time, a morphology transition from a mesh-like pattern to a dense branching morphology (DBM) (Fig. 4) can be observed. Measurements indicate that the morphology transition corresponds to an increase in pH of the electrolyte solution, owing to generation of hydrogen gas. When the morphology changed to DBM, the arches connecting the neighbouring branches disappear and a more uniform envelope emerges. The tips of the branches do not then approach each other.

To study the stream pattern around the growing tips, we used transmission optical dark-field microscopy and interference contrast microscopy to trace the movement of small particles in the electrolyte solution. We find that during mesh formation, the particles flow towards the tips of the branches and those trapped in between the branches flow in circles. In contrast, during the growth of DBM, the small particles move slowly towards the deposit branches and do not circulate. The observations indicate

that connection of the branches is related to interbranch convection.

Recently, Fleury, Chazalviel and Rosso proposed[9] an electroconvection model to explain the arch-shaped concentration distribution in front of the deposit branches. In this model, positive charges are assumed to exist in the liquid just in front of the tip of the branches and the growth speed of the deposit is the speed at which the anions are withdrawn from the deposit. A coulombic force is assumed to act on the deposit tips owing to this local accumulation of electric charge. Two vortices between the neighbouring tips of branches are expected, shown schematically in Fig. 3*e*. The largest loops of the vortices form an arch (the dashed line in Fig. 3*e*), which separates two zones: a depleted zone (the area below the arch) and a zone with constant concentration (above the arch). In the area of constant concentration, the stream lines converge to the tip of branches and there is no circulation; in contrast to the upper region, in the depleted area the flow is circulating. So the electrolyte in the region above the arch cannot enter the lower part by flow, that is, the boundary between these two zones is very sharp if diffusion is ignored.

In reality, however, the ion diffusion widens the virtual interface between the two zones. The arches connecting the neigh-

FIG. 1 The morphology of the iron deposit observed during electrochemical deposition from acidified $FeSO_4$ aqueous solution films. The growth pattern and the evolution of morphology is observed using an optical microscope and recorded by either a video system or a camera. METHODS. The cell for electrochemical deposition consists of two closely spaced microscope glass slides, sandwiching the electrolyte. The thickness of the film is controlled by two mica spacers, varying in thickness from 10 to 120 μm. Two straight, parallel electrodes, (made of iron with purity 99.997% (anode) and a pencil core with rectangular cross-section (cathode)) are fixed on the bottom slide, 22 mm apart. This cell is almost the same as that reported previously[13], except that the gap between the cathode and the edge of the upper glass plate is slightly larger. In this way the hydrogen generated at the beginning of the experiment can be released easily, otherwise the later growth of the iron deposit will be completely blocked by the hydrogen bubbles. Analytical grade $FeSO_4$ (99.5% pure) is used to give a 0.5 M solution; sulphuric acid is added in drops to give a pH of ~2.0. The applied voltage across the two electrodes is 4.000 ± 0.001 V, kept constant during the experiment. (The voltage should not be too high during growth in order to prevent the generation of too many hydrogen bubbles.) The electrodeposition is carried out at room temperature (~20 °C).

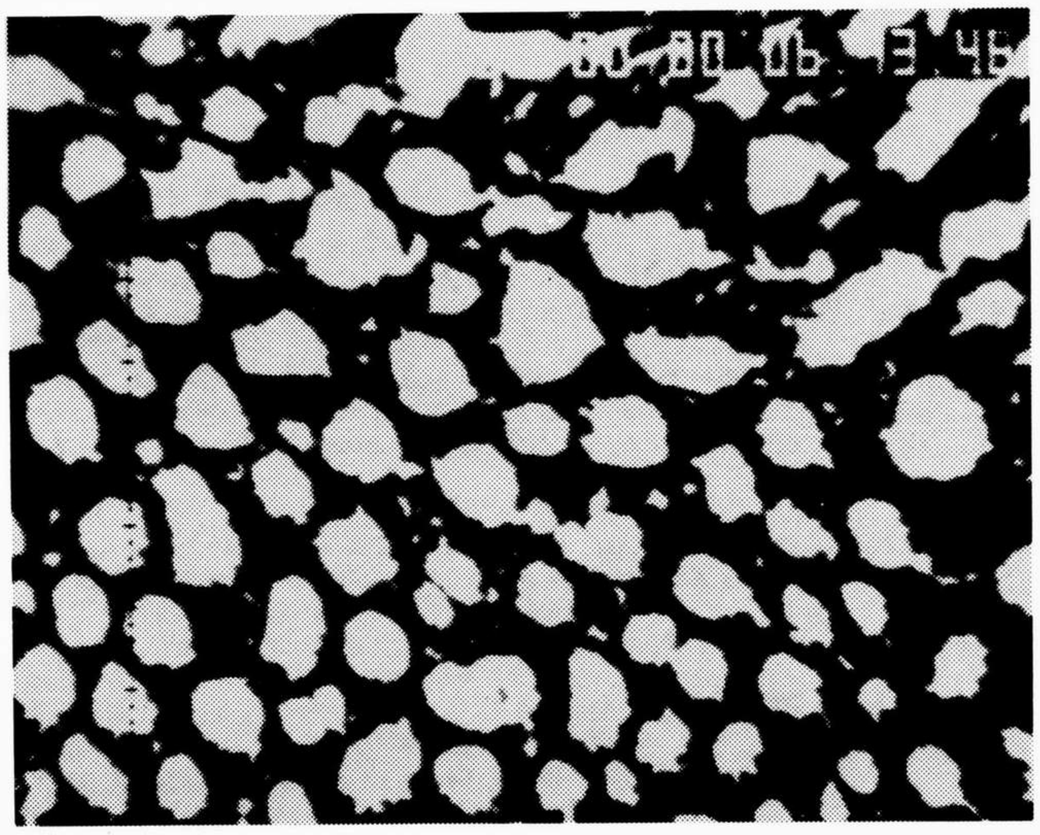

200 μm

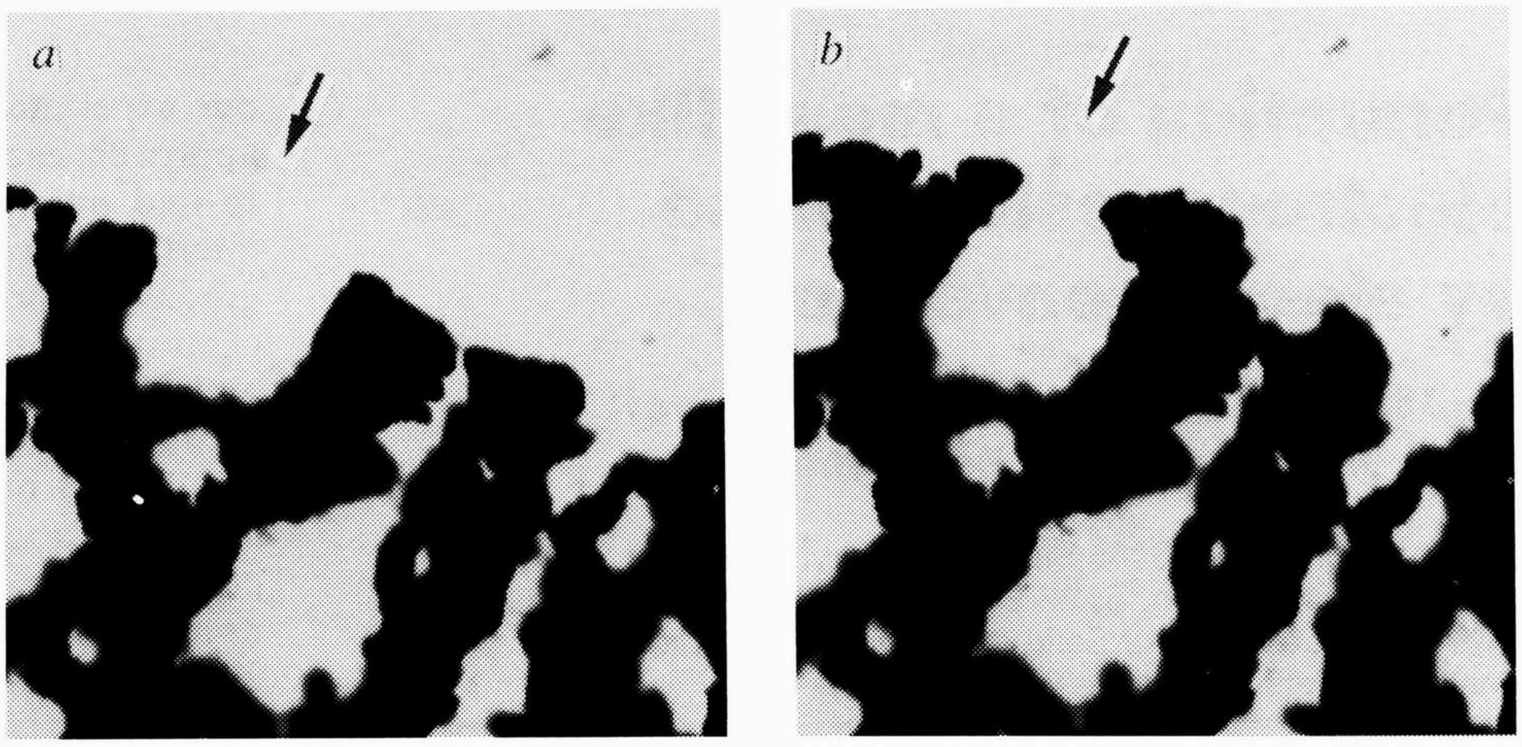

FIG. 2 The netting process during iron electrodeposition (experimental conditions as Fig. 1). As indicated by the arrow, previously separated tips of the deposit branches approach each other (*a*, *b*). When the two tips meet, a circular mesh is formed (*c*), and new branches are generated on the edge of the mesh (*d*). The process goes on, producing a network pattern. The time interval between two successive pictures is ~7 s. The thickness of the electrolyte solution film shown here is 70 μm. The net pattern and its mesh size do not change greatly when the thickness of the electrolyte film is reduced from 120 to 10 μm indicating that the netting phenomenon is not dependent on the geometry of the cell.

100 μm

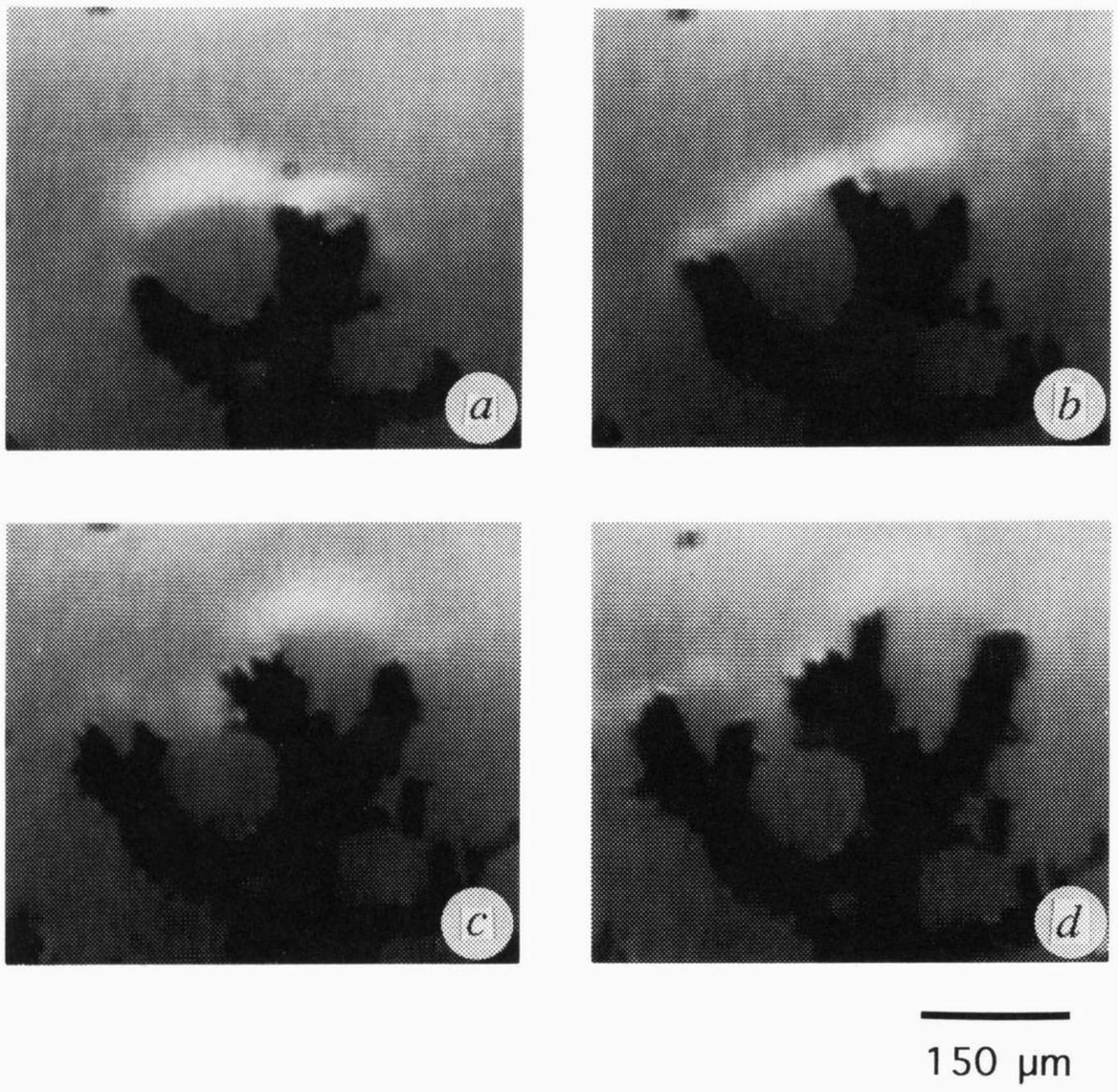

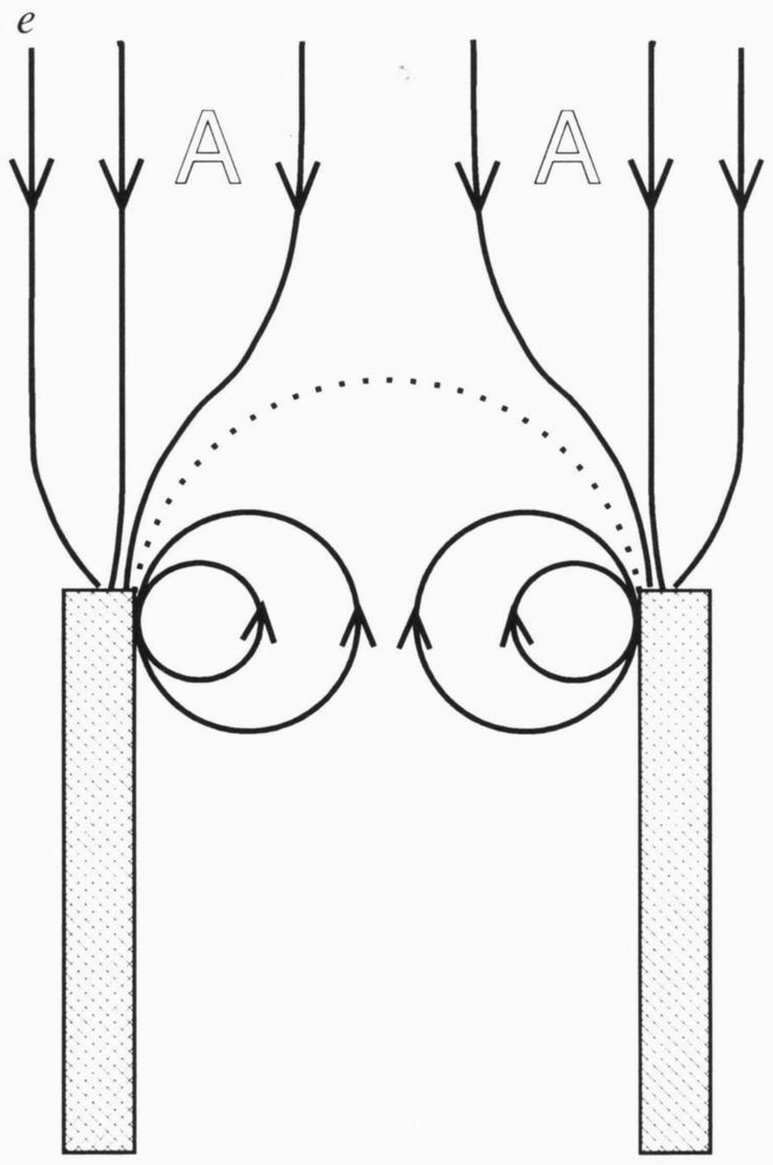

FIG. 3 *a–d*, Interference contrast micrographs of the concentration gradient in front of the growing tips during iron deposition, (experimental conditions as Fig. 1) showing bright arches bridging the neighbouring growing tips of the branches. As the deposit grows, the branches meet each other along the bright arch, the curvature and the contrast of which decreases as the branches approach each other. The arch finally disappears when the tips meet or become very close (*c* and *d*). *e*, Schematic diagram of the stream lines around two neighbouring deposit branches. The dashed line represents the virtual boundary between a zone free of ions (the area below the dashed line) and a zone with constant concentration (above the dashed line). The bright arch shown in *a* reflects the concentration gradient across this virtual boundary. Below the dashed line, the stream lines have the shape of vortices (see text). Transmission optical dark-field microscopy (which can image particles down to 0.1 μm diameter in solution) and interference contrast microscopy are used to visualize the stream pattern by tracing the movement of small particles (possibly $Fe(OH)_2$ or $Fe(OH)_3$)[14] during electrodeposition. During the netting process, the particles are found moving towards the branch tips along the streamlines A; on approaching the tips the velocity of the particles increases considerably. The particles trapped in the depleted area are found to move in circles (see text). The convection and net formation are independent of the solution film thickness and occur also if $FeCl_3$ instead of $FeSO_4$ is used. Therefore these phenomena are not caused by gravity-driven convection and anion chemistry.

bouring branches in Fig. 3*a–d* reflect the concentration gradient across the extended virtual boundary. However, as soon as Fe^{2+} diffused across the boundary, the existing vortices in the depleted region will transport Fe^{2+} ions to the facing parts of the neighbouring tips (Fig. 3*e*). The stream lines of the vortices are converging to the tips of the deposit, so the region on the tip which is facing the neighbouring one has more chance to grow. Consequently, the neighbouring tips tend to approach each other along the arch (Fig. 3). When two tips meet, a 'mesh' is formed. Thereafter, under the influence of the diffusion field and the electric field, new branches will be generated on the edge of the mesh (Fig. 2*d*) and the process described above will repeat. In this way a mesh-like pattern is formed.

For convection to be initiated, a local force acting on the ions in the solution in the vicinity of the tip of the deposit branches is required. Fleury *et al*[9] have suggested that a small excess of metal ions near the tips of deposit branches provide a Coulomb force in an electric field which initiates convective motion. But

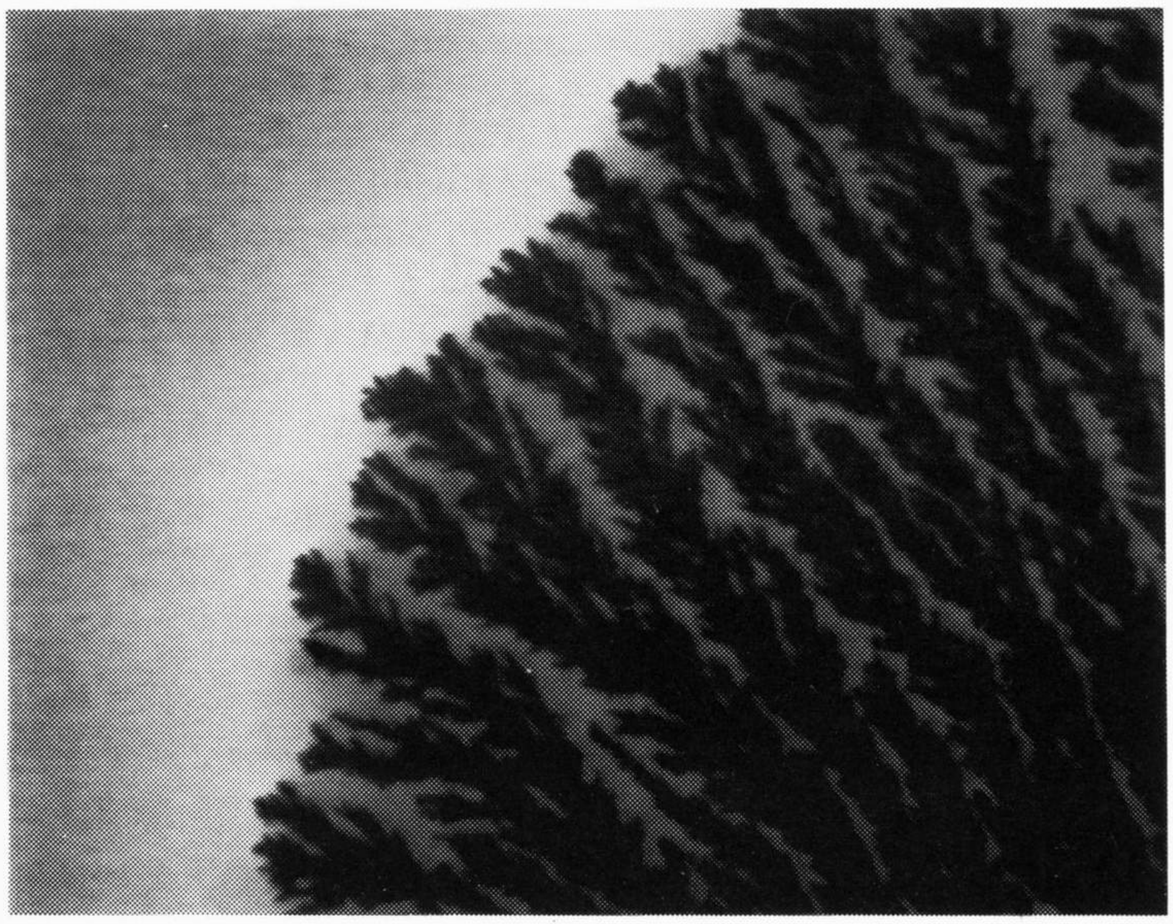

FIG. 4 After continued growth of the 'net-pattern' iron deposit shown in Fig. 1 (typically several millimetres in length), the deposit changes to a dense branching morphology (DBM), shown here as an interference contrast micrograph. There are no bright arches connecting the growing tips and the deposit branches no longer approach each other. Regions of solution with higher contrast (in front of the growing DBM interface) can be seen, showing a concentration gradient in the diffusion field. The concentration field is more uniform now and forms an envelope around the growing pattern. When the growth morphology changes to DBM, the number of the small diffusing particles increases gradually. The particles trapped between the deposit branches do not circulate, which is different from the situation in the earlier net pattern growth (Fig. 3). The pH of the electrolyte solution was found to have increased to ~4.0 after the morphology of the deposit changed to DBM. The time when the morphology changes depends on the initial H_3O^+ concentration and volume of the electrolyte solution, that is, the lower the initial pH and the thicker the aqueous film, the longer the net pattern will grow. The increase of pH is due to hydrogen generation and the consumption of H^+ ions. These experiments indicate that the interbranch convection depends on the H_3O^+ concentration, and the interbranch convection governs the morphology of the deposit.

when deposit growth reaches a stationary state, a depleted zone is expected in front of the growing front, that is, the concentration of metal ion near the growing interface is lower. We therefore suppose that the contribution of the metal ions is small. Instead, we suggest that H_3O^+ ions accumulated around the growing front in our acidified solution are predominantly responsible for convection: during electrodeposition, H_3O^+ plays the role of an impurity and gradually accumulates in front of the growing interface while Fe^{2+} deposits on the cathode. When the concentration of H_3O^+ is sufficiently high, however, hydrogen bubbles will be nucleated, as indeed we observe in our experiments. So the overall H_3O^+ concentration in electrolyte solution decreases gradually as the electrodeposition goes on. Once the H_3O^+ concentration has decreased sufficiently, convection will be suppressed. This attenuation of convection is then responsible for the change of deposit morphology (Fig. 4).

We monitored the electric current during electrodeposition. The current fluctuates greatly and declines slightly during the growth of a mesh-like pattern, whereas it is steady and increases gradually for the DBM growth. The large fluctuation of the electric current may be attributed to the interbranch convection (M.W. *et al.*, manuscript in preparation). There is no great difference in electric current before and after the morphology transition. This may imply that a possible passivation of the anode and/or cathode by increasing the pH of the electrolyte solution does not affect the observed morphology transition. The role of H_3O^+ in stimulating interbranch convection is further supported by electrolysis of a pure H_2SO_4 solution film ($pH \sim 2$), with a graphite anode and inert branched metal needles as the cathode. It is found that if the applied voltage exceeds ~ 3 V, interbranch convection can be detected, either by directly monitoring the movement of intentionally added small particles near the cathodes or by measuring fluctuation of the electric current (M.W. *et al.*, manuscript in preparation).

It was reported recently that Marangoni-like (concentration-gradient-induced) effects on the surface tension at a liquid–liquid interface between the diffusion layer around the tip and the outer region may induce a convective instability even when the interface is not very sharp[12]. In our case, the interfacial tension acting on the boundary separating the regions with different H_3O^+ and Fe^{2+} concentrations may provide a force that is mathematically equivalent to the electric force proposed in ref. 9. But the relative effects of interfacial tension and electric force cannot be distinguished in our experiments. However, the observed convection with stream lines shown in Fig. 3*e* indicates that some force acts, whatever its origin. Our experiments indicate that the formation of the mesh pattern is closely related to the presence of convection. □

Received 14 October 1993; accepted 10 January 1994.

1. Kessler, D. A., Koplik, J. & Levine, H. *Adv. Phys.* **37,** 255–339 (1988).
2. Brady, R. M. & Ball, R. C. *Nature* **309,** 225–229 (1984).
3. Matsushita, M., Sano, M., Hayakawa, Y., Honjo, H. & Sawada, Y. *Phys. Rev. Lett.* **53,** 286–289 (1984).
4. Sawada, Y., Dougherty, A. & Gollub, J. P. *Phys. Rev. Lett.* **56,** 1260–1263 (1986).
5. Grier, D., Ben-Jacob, E., Clarke, R. & Sander, L. M. *Phys. Rev. Lett.* **56,** 1264–1267 (1986).
6. Argoul, F., Arneodo, A., Grasseau, G. & Swinney, H. L. *Phys. Rev. Lett.* **61,** 2558–2561 (1988).
7. Garik, P. *et al. Phys. Rev. Lett.* **62,** 2703–2706 (1989).
8. Melrose, J. R., Hibbert, D. B. & Ball, R. C. *Phys. Rev. Lett.* **65,** 3009–3012 (1990).
9. Fleury, V., Chazalviel, J.-N. & Rosso, M. *Phys. Rev. Lett.* **68,** 2492–2495 (1992); *Phys. Rev.* E**48,** 1279–1295 (1993).
10. Fukunaka, Y., Yamamoto, T. & Kondo, Y. *J. electrochem. Soc.* **136,** 3630–3633 (1989).
11. Wang, M. & Ming, N.-B. *Phys. Rev. Lett.* **71,** 113–116 (1993).
12. Garik, P., Hetrick, J., Orr, B., Barkey, D. & Ben-Jacob, E. *Phys. Rev. Lett.* **66,** 1606–1609 (1991).
13. Wang, M. & Ming, N.-B. *Phys. Rev.* A**45,** 2493–2498 (1992).
14. Cotton, F. A. & Wilkinson, F. R. S. G. *Advanced Inorganic Chemistry* 2nd edn (Wiley, New York 1966).

ACKNOWLEDGEMENTS. This work was supported by the China Science and Technology Committee and the Dutch Ministry of Education.